Effects of Benzo[*a*]pyrene Adduct Stereochemistry on Downstream DNA Replication in Vitro: Evidence for Different Adduct Conformations within the Active Site of DNA Polymerase I (Klenow Fragment)†

Yuriy O. Alekseyev‡ and Louis J. Romano*

Department of Chemistry, Wayne State University, Detroit, Michigan 48202

Received October 10, 2001; Revised Manuscript Received January 18, 2002

ABSTRACT: The presence of bulky adducts in DNA is known to interfere with DNA replication not only at the site of the lesion but also at positions up to 5 nucleotides past the adduct location. Kinetic studies of primer extension by exonuclease-deficient *E. coli* DNA polymerase I (Klenow fragment) (KF) when (+)-*trans*- or (+)-*cis*-B[*a*]P-N^2-dG adducts were positioned in the double-stranded region of the primer-templates showed that both stereoisomers significantly block downstream replication. However the (+)-cis adduct, which causes a stronger inhibition of the nucleotides insertion across from and immediately past the lesion, affected the downstream replication to a much smaller extent than did the (+)-trans adduct, especially when the B[*a*]P-modified dG was properly paired with a dC. The effects of mismatches across from the adduct and the sequence context surrounding the adduct were also dependent on the stereochemistry of the B[*a*]P adduct. Thus, the identity of the nucleotide across from the adduct that provided the best downstream replication was different for the (+)-cis and (+)-trans adducts, a factor that might differentially contribute to the mutagenic bypass of these lesions. These findings provide strong direct evidence that the conformations of the (+)-cis and (+)-trans adducts within the active site of KF are significantly different and probably differentially affect the interactions of the polymerase with the minor groove, thereby leading to different replication trends. The stereochemistry of the adduct was also found to differentially affect the sequence-mediated primer-template misalignments, resulting in different consequences during the bypass of the lesion.

The covalent DNA adducts formed by metabolically activated B[*a*]P[1] have been shown to be strong blocks to DNA replication in vitro, allowing only the infrequent incorporation of a nucleotide across from the modified base and a negligibly small extent of further bypass (*1*−*6*). These lesions are much more readily bypassed in vivo by mechanisms that are still poorly understood (*7*). However, this bypass can lead to nucleotide insertions or deletions and all types of base substitution mutations (*8*), some of which are correlated with tumor initiation and progression (*9, 10*). The mutational spectra caused by these adducts are usually complex and depend primarily on the organism studied, the stereochemistry of the DNA adduct, and the DNA sequence context surrounding the lesion (*2, 7, 11, 12*).

† This investigation was supported by U.S. Public Health Service Grant CA40605 awarded by the Department of Health and Human Services.

* To whom correspondence should be addressed. Tel.: 313-577-2584. Fax: 313-577-8822. E-mail: LJR@chem.wayne.edu.

‡ Present address: Division of Bioengineering and Environmental Health, Massachusetts Institute of Technology, Cambridge, MA 02139.

[1] Abbreviations: B[*a*]P, benzo[*a*]pyrene; *anti*-B[*a*]PDE, benzo[*a*]-pyrene diol epoxide or r7,t8-dihydroxy-t9,10-epoxy-7,8,9,10-tetrahydrobenzo[*a*]pyrene; KF, Klenow fragment; (+)-*anti*-B[*a*]PDE, 7(*R*), 8(*S*), 9(*S*), 10(*R*) absolute configuration; (−)-*anti*-B[*a*]PDE, 7(*S*), 8(*R*), 9(*R*), 10(*S*) absolute configuration; B[*a*]P-N^2-dG, benzo[*a*]pyrene adduct at N-2 position of guanine; PAGE, polyacrylamide gel electrophoresis; K_M, Michaelis constant; V_{max}, maximum rate of reaction; F_{ins}, frequency of insertion; F_{ext}, frequency of extension; AAF, *N*-acetyl-2-aminofluorene; AF, *N*-2-aminofluorene; dNTP, 2′-deoxynucleotide triphosphate; K_d, dissociation constant.

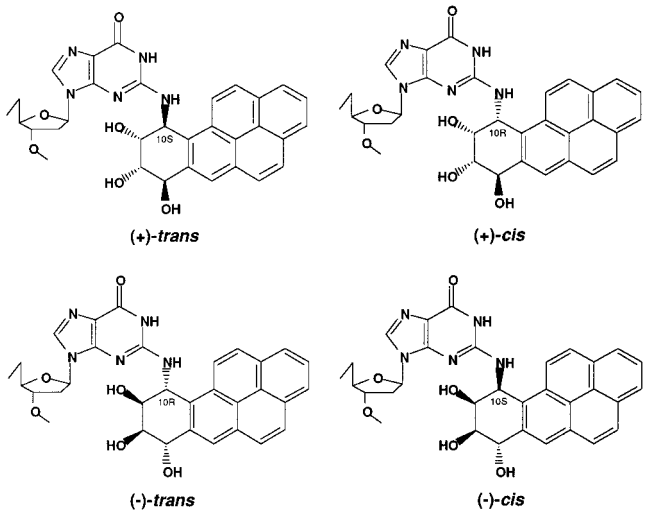

FIGURE 1: Structures of (±)-*anti*-B[*a*]P-N^2-dG adducts.

(±)-*anti*-B[*a*]BDE, the most biologically relevant active metabolite of B[*a*]P (*13*), reacts predominantly with the exocyclic amine (N2) of guanine in duplex DNA via the cis or trans opening of the epoxy ring at the C-10 position to form four adducts (Figure 1) (*9*). The structures of these adducts in the DNA duplex and at a primer-template junction have been studied using NMR and by other spectroscopic and computational methods [reviewed in (*14*)]. These studies showed that the cis and trans adducts adopt strikingly

10.1021/bi015850l CCC: $22.00
Published on Web 03/06/2002

different conformations in double-helical DNA. The NMR data suggest that the pyrenyl moiety of the trans adducts positioned within the 5′-CGC-3′ sequence context is located in the minor groove of the DNA helix, whereas the modified guanine is in partial hydrogen-bonded alignment with the partner cytosine. Conversely, the major conformers of both cis adducts are intercalative, and the modified and partner bases are displaced outside the DNA helix.

There is also a dramatic change in the structure of the (+)-trans adduct located at a primer-template junction when the primer is extended from a position one nucleotide before the adduct to a position that terminates across from the adduct. When the primer is terminated before the adduct, the pyrenyl moiety is stacked with the last base pair of the double-stranded segment of the primer-template, such that the modified guanine is displaced toward the major groove and adopts syn conformation (*15*). In contrast, when the primer is extended and contains a cytosine across from the adduct (*16*), the pyrenyl ring is positioned on the minor groove side of the primer-template, pointing toward the 5′ end of the template strand. The modified base in this case retains the anti glycosidic torsion angle and is in partial Watson−Crick hydrogen-bonded alignment with the complementary cytosine (*16*). Overall this structure resembles that of the same adduct in the fully complementary duplex.

Although the structures of these adducts in duplex DNA have been well studied, there is very little information available regarding their structures in the active site of a DNA polymerase, how these adducts affect the interactions of the DNA with the polymerase, or if adducts with different stereochemistry affect these interactions differentially. One report directly relating to this question is an analysis in which a molecular dynamics simulation was carried out using rat DNA polymerase β complexed with primer-template DNA containing the major (+)-*trans*-*anti*-B[*a*]P-N^2-dG adduct (*17*). The primer in this study was terminated before the adduct position, and the pyrenyl ring was found to be stacked with the last base pair of the double-stranded segment of the primer-template, resembling the above-mentioned NMR structure (*15*), except that the modified guanine retained the anti conformation. A second computational study suggested a different structure for the (+)-*trans*-B[*a*]P-N^2-dG adduct positioned within the active site of the T7 DNA polymerase (*18*). In this study, the primer was terminated before the adduct, and the simulation was carried out in the presence of the most commonly incorporated nucleotide, dATP. The structure that was determined showed the modified dG in a syn conformation and the B[*a*]P moiety positioned in the major groove, thus allowing the incoming dATP to be accommodated.

In the absence of sufficient information about the structures of adducts of different stereochemistry within the active site of a polymerase, there have been numerous indirect studies that have attempted to explain differential effects of the bulky lesions on DNA replication by correlating the structures of these adducts in double-stranded DNA or at a primer-template junction with the mutagenic event that a particular isomer induces [reviewed in (*7*)]. For example, it has been hypothesized that the DNA polymerase can trap the adduct in a specific conformation that is presumably determined by the conformation prevailing in the double-helical DNA before the opening of the replication fork and that mutagenic properties of the lesion depend on the nature of this trapped conformation (*8, 19*). However, the assumption that the structure of the adduct in the active site of the polymerase maintains a relationship to the structure in duplex DNA comes with the caveat that the conformation in the active site may be affected by constraints imposed by accommodating the bulky adduct in the rather tight polymerase active site and/or that the adduct conformation might be changed as a result of this accommodation (*18*).

In vitro studies have shown that the cis adducts are stronger blocks of replication than the trans adducts during incorporation of a dNTP across from the adduct (*1, 5*), as well as at the position immediately following the adduct (*5*). However, the order of the preference of the dNTP that is incorporated across from the adduct and the identity of the nucleotide across from the adduct that best allows further extension were found to be independent of the adduct stereochemistry (*1, 5*). These facts make it difficult to use this type of data as a guide in determining how a DNA polymerase interprets different adduct structures during replication.

We have begun to develop methods to address this problem that are based on attempting to measure differences in the interactions of the polymerase with primer-templates containing bulky adducts of different structures. For example, we have used a gel retardation assay (*20, 21*) and a limited trypsin digestion analysis (*22*) to show that that bulky lesions, such as B[*a*]P, AF, and AAF adducts, can be well accommodated within the active site of the polymerase in the open binary complex, but that these adducts can interfere with conformational change of the polymerase to the closed catalytically active ternary complex. Presumably these bulky structures alter the structure and stability of the ternary complex (*20*−*22*), thus affecting an important step that is crucial in determining the fidelity of the nucleotide incorporation step (*23*). We have also showed that the (+)-*cis*- and (+)-*trans*-*anti*-B[*a*]P-N^2-dG adducts in the 5′-CGT-3′ sequence affect the binding of the KF to primer-templates differently if the primer extends to the position across from the adduct, a result that suggests that the conformations of these two stereoisomers within the active site may be indeed different (*21*). Despite these differences, synthesis past each of these stereoisomers by KF on these primer-templates was allowed only when dT was positioned across from the adduct (*5*), suggesting that replication at this position depends on the identity of a nucleotide positioned across from the adduct rather than the stereochemistry of the adduct.

In the present study, primer-templates with primers that extended to the +1 position past the adduct were used to compare the effect of B[*a*]P adduct stereochemistry on nucleotide incorporation at the +2 position. Although both adducts inhibited incorporation at this position, the (+)-cis adduct affected the downstream replication to a much smaller extent than did the (+)-trans adduct, especially when the B[*a*]P-modified dG was properly paired with a dC. The identity of a nucleotide positioned across from the adduct that had the least inhibitory effect on downstream replication was different for the (+)-cis and (+)-trans adducts. These data provide strong direct evidence that the conformations of the (+)-cis and (+)-trans adducts within the polymerase are significantly different.

MATERIALS AND METHODS

Materials. The Klenow fragment of *E. coli* DNA polymerase I [D355A, E357A double mutant (*24*)], T4 polynucleotide kinase, and T4 DNA ligase were purchased from Amersham Pharmacia Biotech. Oligonucleotides were obtained from Midland Certified Inc. and Operon Technologies. dNTPs were purchased from Promega. [γ-^{32}P]ATP was from ICN Biomedicals. The racemic (±)-*anti*-B[*a*]PDE was purchased from the National Cancer Institute Chemical Reference Standard Repository (Kansas City, MO). All other general reagents and chemicals were obtained from Fisher and VWR.

Synthesis and Purification of the B[a]PDE-Modified Oligonucleotides. All oligonucleotides were purified by 20% denaturing polyacrylamide gel electrophoresis (PAGE) in the presence of 8 M urea according to the procedures described in (*25*) and desalted with Centricon-3 microconcentrators (Amicon) according to the manufacturer's protocol. The 11-mers were modified by racemic (±)-anti-B[*a*]PDE as described (*26*). Briefly, 50−80 ODUs of 11-mer oligonucleotide in 100 μL of 10 mM potassium phosphate buffer (pH 7.0) was mixed with 150 μL of a 5.5 mM solution of (±)-*anti*-B[*a*]PDE in tetrahydrofuran/triethylamine (19:1). After 48 h, the four stereoisomers [obtained in the following approximate relative yields: (+)-trans:(−)-trans:(+)-cis:(−)-cis = 5.5:3.5:1:0.5] were separated by reverse-phase HPLC, gel-purified, and desalted under conditions described in (*26*). The modified oligonucleotides were characterized by UV and CD spectroscopy, and the purity was assessed by denaturing electrophoresis and HPLC analysis as described in (*26*).

The 11-mers with (+)-*trans*- and (+)-*cis*-B[*a*]P-N^2-dG adducts, as well as unmodified 11-mers, were ligated to the phosphorylated 17-mer, using fully complementary 22-mers as scaffolds according to the manufacturer's protocol (Amersham Pharmacia Biotech), and the ligated 28-mers were separated from the ligation mixture using 20% denaturing PAGE and desalted as described in detail (*5*, *21*).

Kinetics of Nucleotide Insertion. The time course analyses were performed under conditions similar to those described (*5*). The purified 24-mers (10 pmol) were 5′-end-labeled with T4 polynucleotide kinase and [γ-^{32}P]ATP and purified using 20% PAGE in the presence of 8 M urea (the labeled DNA was detected by Molecular Dynamics Phosphor Imager Storm), the corresponding bands were cut out and eluted overnight, and the solution was desalted using Centricon-3 microconcentrators (Amicon). The modified 28-mer templates (final concentration 8 nM) were annealed to the ^{32}P-labeled 24-mer primers in a 4:1 molar ratio by heating to 95 °C and slow-cooling to room temperature in a 50 μL volume containing 50 mM Tris-HCl, pH 7.5, 10 mM $MgCl_2$, 1 mM dithiothreitol, and 0.05 mg/mL bovine serum albumin. Under these conditions, the labeled primer is completely annealed, which was confirmed by analysis of an aliquot taken from the annealing mixtures using a 7% native PAGE analysis at +4 °C according to the procedure described in (*5*). After addition of KF (final concentration 0.02 unit/μL) and 400 μM of the next correct dATP, 8 μL aliquots were removed from the reaction mixtures at the indicated times. To estimate if the primer-templates are properly aligned, primer extension experiments were performed in the presence of incorrect dNTPs, all four dNTPs, or a combination of two dNTPs, and higher amounts of the enzyme (final concentration up to 0.08 unit/μL) and longer reaction times (up to 24 h) were used. The samples were then heated for 3 min at 95 °C in the presence of formamide and analyzed using 15% denaturing PAGE (0.4 mm). Band intensity was determined using a Molecular Dynamics Storm PhosphorImager.

Gel Retardation Assay. Equilibrium dissociation constants (K_d) for the polymerase−primer-template complexes were determined as described (*21*). Briefly, increasing amounts of KF (ranging from 0 to 200 nM) were incubated with ^{32}P-labeled primer-templates (5−50 pM) for 30 min at room temperature in 50 mM Tris-HCl, pH 7.5, containing 10 mM $MgCl_2$, 1 mM dithiothreitol, 0.05 mg/mL bovine serum albumin, and 4% glycerol. The incubation mixtures were analyzed in a native 7% polyacrylamide gel preequilibrated with 36 mM Tris−borate buffer, pH 8.3. Quantification of the gels was performed using Molecular Dynamics PhosphorImager Storm and ImageQuant. The amount of protein−DNA complex formed at equilibrium was calculated as the difference in the band intensities of the initial primer-templates without polymerase addition and unbound primer-templates. To determine K_d, the fraction of the DNA bound to the protein was plotted against the initial protein concentrations, and the data were analyzed using Ultrafit (Biosoft, Cambridge, U.K.) by fitting to the equation for single-site ligand binding. Each determination represents the average of at least three independent experiments.

RESULTS

A kinetic analysis of the replication bypass of a DNA adduct typically involves the determination of individual insertion frequencies of nucleotides across from the lesion and the extension frequency of further bypass in the presence of the next correct nucleotide from a primer that contains one of the four possible nucleotides across from the adduct (*27, 28*). The product of these two parameters is used to estimate the overall efficiency of lesion bypass (*1*). However, this type of analysis may be incomplete since it has been shown that bulky adducts can interfere with DNA synthesis at positions as far as five nucleotides downstream from the modified nucleotide (*29*). In addition, the presence of a bulky adduct has been shown to promote primer-template misalignments, which also might affect the results of the primer-extension analysis (*1, 6*). In the present study, we have begun to analyze effects of adduct stereochemistry and DNA sequence both on nucleotide incorporation downstream from the lesion and on the formation of misaligned DNA structures.

Effect of Adduct Stereochemistry on Downstream Primer Extension. Previous studies have shown that the (+)-*trans*- and (+)-*cis*-*anti*-B[*a*]P-N^2-dG adducts are strong blocks of replication when the primer is terminated upstream from the adduct and are especially strong when the primer terminates across from the modified guanine (*1, 2, 5*). Figure 2 shows the results of synthesis when the primer terminates one nucleotide past the adduct (+1 position) and positions a dC across from the modified guanine. Compared with an unmodified template, where extension under these conditions occurs in seconds (data not shown), incorporation at the +2 position of the primer is significantly affected if either a (+)-cis or a (+)-trans adduct is present. Interestingly, the presence

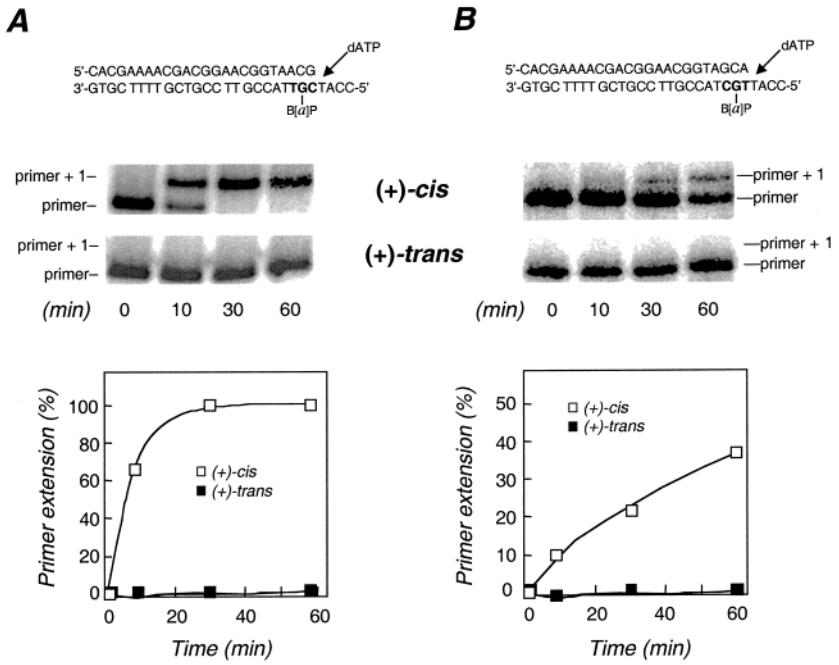

FIGURE 2: Time course of primer extension past the (+)-*trans*- and (+)-*cis*-B[*a*]P-N^2-dG adducts paired with dC in (A) 5′-CGT-3′and (B) 5′-TGC-3′ sequence contexts by KF. The ^{32}P-labeled 24-mer primers positioning dC across from the adduct were annealed to 28-mer templates and incubated with KF in the presence of the next correct nucleotide (dATP) under conditions described under Materials and Methods. Aliquots were taken from the reaction mixture at the indicated time points, heated in the presence of formamide, and analyzed by denaturing PAGE (15%). Primer extension (%), calculated as the ratio of the band intensity of the extension product (primer +1) to that of the total DNA (an average of three independent experiments), was plotted as a function of time.

of the (+)-trans adduct essentially completely inhibited incorporation, whereas the blocking effect of the (+)-cis adduct was significantly less (Figure 2 and Table 1). For example, in the case of the 5′-CGT-3′ sequence context, essentially no extension was obtained after a 1 h incubation whereas the (+)-cis adduct is fully extended in less than 30 min (Figure 2A). The blocking effect of the (+)-cis stereoisomer was somewhat greater when the adduct was positioned in the 5′-TGC-3′ sequence context (Figure 2B), where only 38% yield was obtained after 1 h of incubation, while the (+)-trans isomer in the 5′-TGC-3′ sequence again almost completely inhibited downstream replication (Table 1).

Downstream Extension from Primers Having Mismatches Across from the Modified Guanine. Positioning each of the four nucleotides in the primer opposite either the (+)-*cis*- or the (+)-*trans*-B[*a*]P-modified guanine resulted in dramatic differences in the rates of downstream incorporation (Figure 3 and Table 1). In the case of the 5′-CGT-3′ sequence, either a dC or a dT positioned across from for the (+)-cis adduct gave approximately equivalent rates of incorporation of dATP, the next correct nucleotide, both attaining 100% extension in less than 60 min. Placing a purine across from the (+)-cis adduct gave much slower rates of incorporation (only 32% and 7% yields were attained in 1 h in cases of dA or dG positioned across from the adduct, respectively). The order of preference for the nucleotide across from the (+)-cis adduct was dC > dT > dA > dG (Table 1 and Figure 3A, left graph). The (+)-trans isomer gave slow rates of incorporation for all cases, with the extent of primer extension never exceeding 20% in 1 h for any case (Table 1 and Figure 3A, right graph). Interestingly, in the case of the (+)-trans adduct, extension of the primer-templates containing a mismatch across from the adduct was faster compared with fully complementary primer-templates, where extension did not exceed 1% after 1 h. In the best case, where dA was positioned across from the (+)-trans adduct, primer extension reached a 19% yield after 1 h of incubation (Table 1).

When similar experiments were carried out in the 5-TGC-3′ sequence context (Figure 3B), it was also found that the (+)-trans isomer was a stronger block to downstream replication compared with the (+)-cis isomer. However, in this sequence, the order of preference for the nucleotide across from the adduct was somewhat different. For the (+)-cis isomer, dC remained the preferred base to be positioned across from the adduct (38% yield after 1 h), but dT was now the least preferred, attaining only 10% extension in 1 h (Table 1 and Figure 3B, left graph). For the (+)-trans isomer, dA was the preferred base (12% yield after 1 h), and negligibly slow extension (less than a 5% yield) was observed for any of the other nucleotides (Table 1 and Figure 3B, right graph).

Finally, in the experiments shown in Figure 3, the rates of extension were too slow to allow a precise determination of the kinetic parameters and a calculation of the overall reaction efficiencies (V_{max}/K_m). However, the analysis of the time courses in identical experimental conditions allows a qualitative comparison of the trends of the bypass efficiency. In our previous studies, these trends were always correlated with the trends of the values calculated for the overall reaction efficiencies (V_{max}/K_m) (*5*).

Binding of KF to Modified Primer-Templates. To further investigate how the presence of an adduct affects the replication downstream of the lesion, we determined dissociation constants for the binding of KF to the 24-mer/28-mer unmodified primer-templates and the primer-templates containing the (+)-*trans*- and (+)-*cis*-B[*a*]P-N^2-dG adducts within the 5′-CGT-3′ sequence context [shown in Figure 3A

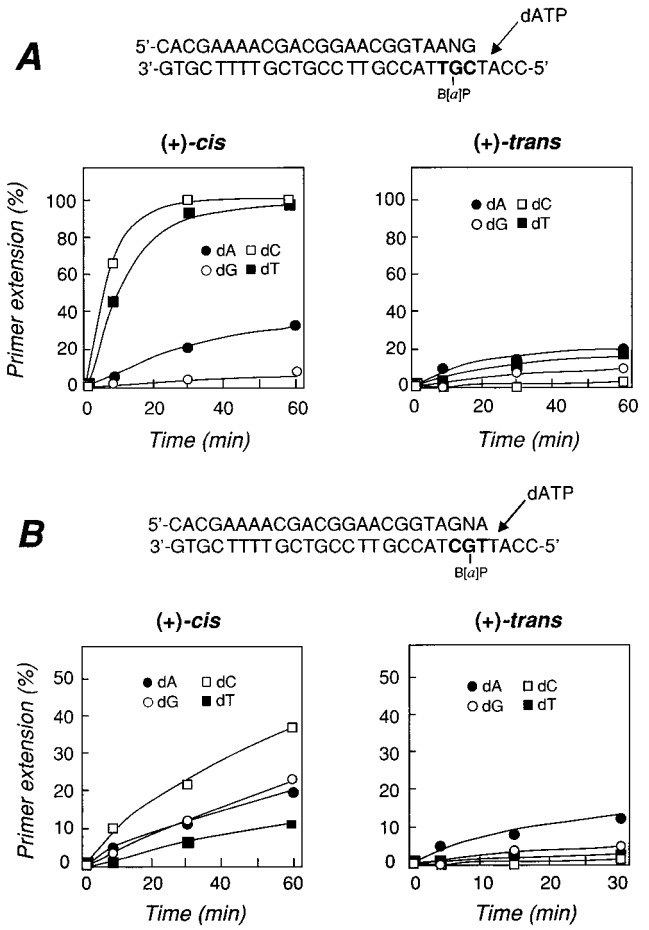

FIGURE 3: Time course of primer extension past the (+)-*trans*- and (+)-*cis*-B[*a*]P-N^2-dG adducts in (A) 5′-CGT-3′ and (B) 5′-TGC-3′ sequence contexts by KF. The ^{32}P-labeled 24-mer primers with one of the four nucleotides (N) across from the adduct were annealed to 28-mer templates and incubated with KF in the presence of the next correct nucleotide dATP under conditions described under Materials and Methods. Aliquots were taken from the reaction mixture at the indicated time points, heated in the presence of formamide, and analyzed by denaturing PAGE (15%). Examples of the corresponding gels are shown in Figure S1 (Supporting Information). Primer extension (%), calculated as a ratio of the band intensity of the extension product (primer +1) to that of the total DNA (an average of three independent experiments), was plotted as a function of time.

Table 1: Primer Extension Yields (%) in the Presence of the Next Correct dNTP[a]

		N[b]			
sequence	adduct	dC	dT	dA	dG
5′-CGT-3′	(+)-trans	1	17	19	8
5′-CGT-3′	(+)-cis	100	100	32	7
5′-TGC-3′	(+)-trans	1	2	12	4
5′-TGC-3′	(+)-cis	38	10	19	21

[a] Reactions were carried out for 1 h. Primer extension yields (%) were calculated as the ratio of band intensity of the extension product to that of the total DNA (average of three independent experiments). The standard deviation in all cases did not exceed 10% and is omitted for clarity. Representative gels are shown in Figures 2 and S1 (Supporting Information). [b] Nucleotide in primer across from the adduct as indicated in Figure 3A, top.

(top)]. Binding to these primer-templates was less stable than when shorter primers were used (*21*), presumably because of the shorter single-stranded 5′-overhangs (discussed in ref *21*). Although binding to the unmodified primer-template was strongest when the primer was correctly paired, much smaller differences were observed for binding to the primer-template that positions any base across from either the (+)-trans or the (+)-cis adduct (Table 2). The stability of the modified complexes followed approximately the same trends as in the case of a primer terminated at the adduct position (*21*): the complexes containing the purines across from the (+)-trans adduct were more stable than those containing the pyrimidines, while complexes with the (+)-cis adducts were more stable when pyrimidines were positioned across from the adduct. The observed differences, however, were small (maximum 1.7-fold), suggesting that these binding differences are not a major factor determining the differences in replication efficiencies observed for the (+)-cis and (+)-trans adducts.

Table 2: Dissociation Constants (nM) for KF Complexes with 24-mer/28-mer Primer-Templates[a]

	N[b]			
template	dC	dT	dA	dG
unmodified	6	14	38	19
(+)-trans	40	35	30	30
(+)-cis	26	25	42	30

[a] Dissociation constants were determined using a gel-retardation assay as described under Materials and Methods using the primer-templates shown in Figure 3A, top. Each determination represents the average of three independent experiments. The standard deviation in all cases did not exceed 50% and is omitted for clarity. [b] Nucleotide in primer across from the adduct as indicated in Figure 3A, top.

Analysis of Primer-Template Misalignments in the 5′-CGT-3′ Sequence. It is theoretically possible that the differences observed in Figures 2 and 3 may be due to different abilities of the cis vs the trans adduct to promote the formation of misaligned structures, such as those shown in Figure 4. For example, misalignment of the 5′-CGT-3′ primer-template as shown in Figure 4A would cause the next correct nucleotide to be dGTP, rather than dATP. If the trans (but not the cis) adduct promoted this misalignment, then addition of dATP should be slow in this case since dGTP would be the correct nucleotide. To test this possibility, the rate of extension in the presence of the next correct nucleotide according to correct alignment (dATP in this case) was compared with the rate of extension in the presence of dGTP, which would be a correct dNTP when this primer-template is misaligned (see Figure 4). The absence of extension in the presence of dGTP would be strong evidence that misalignment had not occurred. The appearance of the primer extension product in the presence of dGTP, on the other hand, would suggest misalignment but would not be absolutely conclusive because the equilibrium between properly aligned and misaligned primer-templates might be shifted by the presence of an excess of corresponding dNTP (*23*). In addition, the fidelity of the dNTP incorporation at the analyzed positions can also be affected by the presence of the upstream adduct that could lead to incorporation of a mispaired dNTP. Additional data were obtained from an analysis of primer-extension in the presence of all four dNTPs and using combinations of two dNTPs.

The analysis presented in Figure 5 for the 5′-CGT-3′ sequence indicates that neither the cis nor the trans adduct promotes a misaligned primer-template structure when dC is present opposite the adduct, and thus the differences

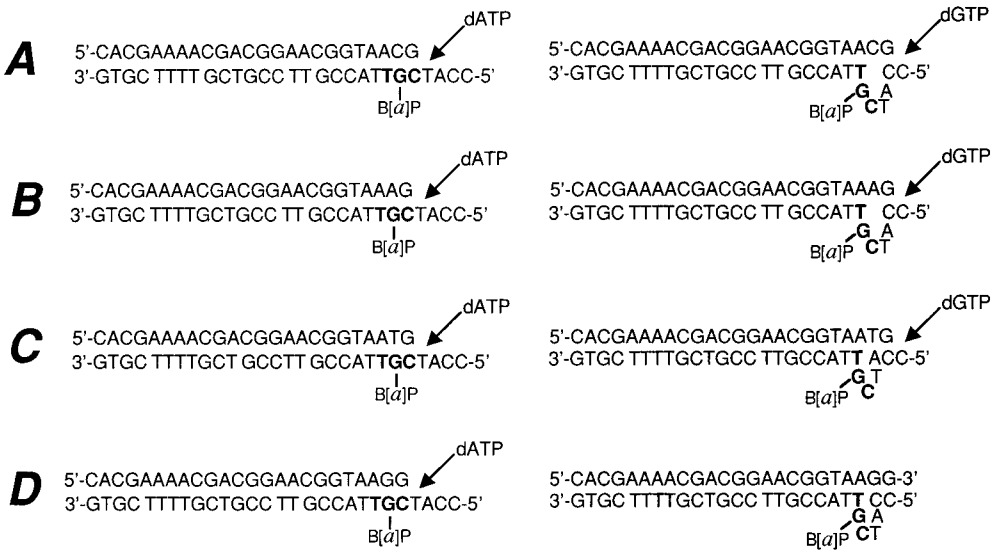

FIGURE 4: Correct and predicted incorrect alignment of primer-templates containing B[*a*]P-N^2-dG adduct in the 5′-CGT-3′ sequence context in which each of the four nucleotides is positioned across from the adduct. Also shown is the next correct dNTP according to the alignment indicated.

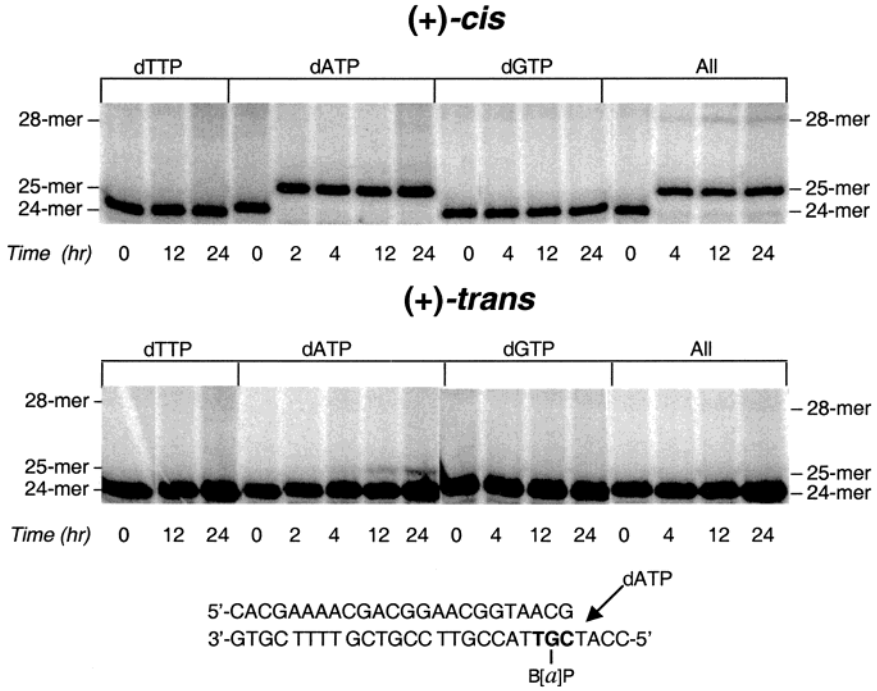

FIGURE 5: Analysis of the primer-template alignment for the (+)-*cis*- or (+)-*trans*-B[*a*]P-N^2-dG adducts in the 5′-CGT-3′ sequence paired with dC. The ^{32}P-labeled 24-mer primers with dC across from the adduct were annealed to 28-mer templates and incubated with KF in the presence of the next correct nucleotide (dATP), an incorrect dNTP (dTTP or dGTP), or all four dNTPs (as indicated) under conditions described under Materials and Methods. Aliquots were taken from the reaction mixture at the indicated time points, heated in the presence of formamide, and analyzed by denaturing PAGE (15%). The products were assigned in accordance with migration of standard oligonucleotides of identical sequences (not shown). Shown below is the correct primer-template alignment that is predicted from the gel analysis.

observed in Figure 2A cannot be explained by different alignment of the primer-templates. In both cases, extension occurs only in the presence of dATP, which is the correct nucleotide to be incorporated for a properly aligned structure (Figure 4A), and not in the presence of any other dNTP (Figure 5 and Table 3). Extension in this case resulted in 100% and 9% yields after a 1 h incubation for the cis and trans adducts, respectively. Although not shown, the addition of dATP and dTTP together (the next two correct dNTPs) resulted in the formation of 25-mer and 26-mer products also in accordance with correct alignment. Simultaneous addition of all four dNTPs gave rise to a fully extended 28-mer product [16% and 2% yield after 24 h for the (+)-cis and (+)-trans adducts, respectively], also indicating that misalignment had not occurred. The formation of the 25-mer product in the presence of all four dNTPs cannot be the result of extension of the misaligned primer-template shown in Figure 4A because the incorporation of dGTP, which would be the next correct dNTP in this case, was not observed (Figure 5 and Table 3). In addition, the formation of a 25-mer product was also observed in the presence of all four dNTPs in the case of the 5′-TGC-3′ sequence (see Figure

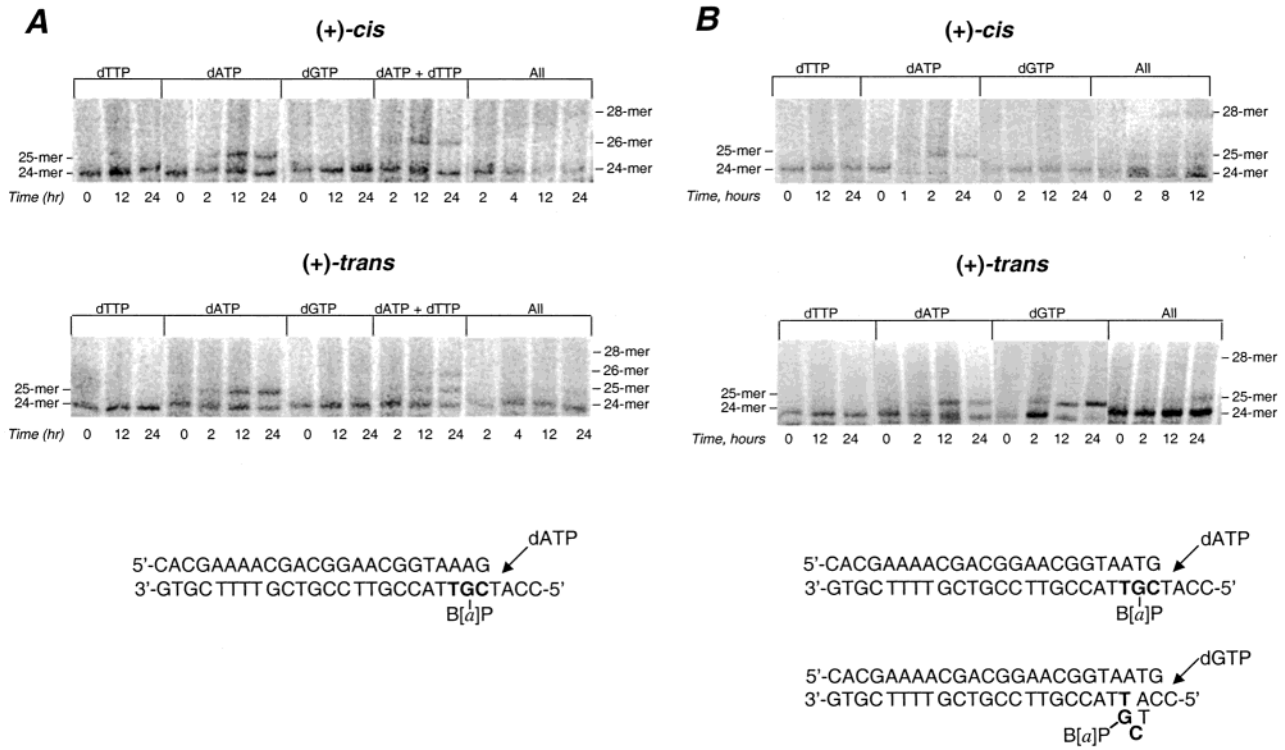

FIGURE 6: Analysis of the primer-template alignment for the (+)-*cis*- or (+)-*trans*-B[*a*]P-N^2-dG adducts in the 5′-CGT-3′ sequence paired with dA (A) or dT (B). The ^{32}P-labeled 24-mer primers positioning dA (A) or dT (B) across from the adduct were annealed to 28-mer templates and incubated with KF in the presence of the next correct nucleotide (dATP), an incorrect dNTP (dTTP or dGTP), a combination of the two next correct dNTPs (dATP and dTTP), or all four dNTPs (as indicated) under conditions described under Materials and Methods. Aliquots were taken from the reaction mixture at the indicated time points, heated in the presence of formamide, and analyzed by denaturing PAGE (15%). The products were assigned in accordance with migration of standard oligonucleotides of identical sequences (not shown). A correct primer-template alignment (as shown in panel A) is predicted from the gel analysis when the adduct is paired with dA. The correct and incorrect primer-template alignments (as shown in panel B) are predicted when the (+)-trans adduct is paired with dT. Only correct alignment is predicted for templates containing the (+)-cis adduct paired with dT.

7), while a misalignment in this sequence would lead to formation of a 27-mer and not a 25-mer. This shorter product is most probably formed because of strong inhibition of replication at this position by the upstream adduct in both sequences. Consistent with the results shown in Figure 2A, the (+)-trans isomer inhibited replication much more strongly than the (+)-cis isomer (Figure 5 and Table 3), so that the full-length extension 28-mer product did not exceed 2% after 24 h and was detectable only on overexposure of the gel (not shown).

The experiment shown in Figure 5 was repeated using primers that positioned dA and dT across from either the (+)-cis or the (+)-trans adducts (Figure 6). With dA positioned across from either adduct, primer extension was detected only in the presence of dATP [52% and 47% yields after 24 h for the cis and trans adducts, respectively (Table 3 and Figure 6A)], indicating that the potential misalignment shown in Figure 4B was not occurring. Addition of the two next correct dNTPs lead to formation of a 26-mer, also in accordance with correct alignment. Full-length extension to a 28-mer occurred at low levels in the presence of all four dNTPs (17% yield for the cis and 8% yield for the trans adduct after 24 h). Similar results were observed when dT was positioned across from the (+)-cis adduct, although the level of 28-mer formed was higher—28% after 24 h (Table 3 and Figure 6B, top gel). However, when dT was positioned across from the (+)-trans adduct (Figure 6B, bottom gel), the rates of primer extension in the presence of dGTP and dATP were comparable (64% yield vs 45% after 24 h, respectively), suggesting that partial primer-template misalignment as shown in Figure 4C may occur. Consistent with this, a very small amount of 28-mer (only a 9% yield vs a 28% yield for the cis adduct) was detected in this case after

Table 3: Analysis of the Primer-Template Misalignment in the 5′-CGT-3′ Sequence

N[a]	adduct	incorpn of dAMP, %[b]	incorpn of dGMP, %[b]	fully extended product, %[c]	alignment
C	(+)-cis	100	ND[d]	16	correct
	(+)-trans	9	ND	2	correct
A	(+)-cis	52	ND	17	correct
	(+)-trans	47	ND	8	correct
T	(+)-cis	100	ND	28	correct
	(+)-trans	45	64	9	cor/incor

[a] Base across from adduct. [b] Primer extension yields (%) in the presence of the next correct dNTP according to correct or incorrect alignment of the primer-template (dATP or dGTP, respectively, as shown in Figure 4) after 24 h of incubation. Primer extension yield (%) was calculated as the ratio of band intensity of the extension product to that of the total DNA (average of three independent experiments). The standard deviation in all cases did not exceed 15% and is omitted for clarity. Representative gels are shown in Figures 5 and 6. [c] Full-length primer extension yields (%) in the presence of all four dNTPs after 24 h of incubation were calculated as the ratio of band intensity of the full-length extension product (28-mer) to that of the total DNA (average of three independent experiments). The standard deviation in all cases did not exceed 20% and is omitted for clarity. Representative gels are shown in Figures 5 and 6. [d] ND: Not detected.

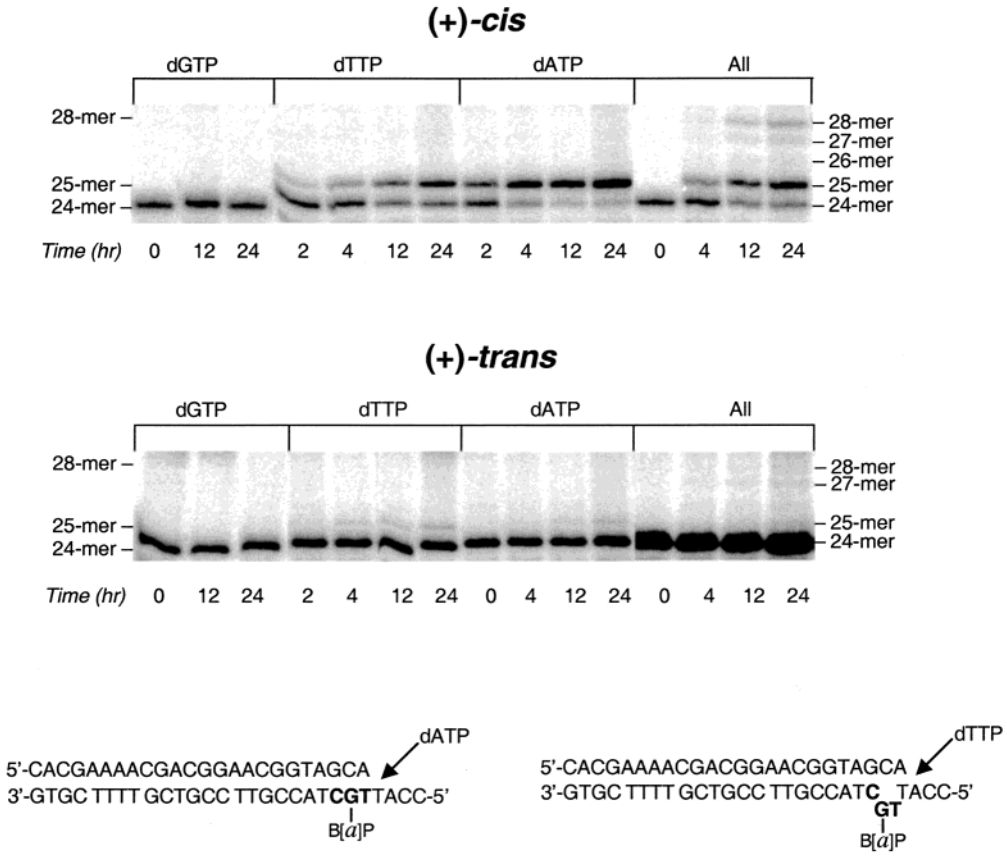

FIGURE 7: Analysis of the primer-template alignment for the (+)-*cis*- or (+)-*trans*-B[*a*]P-N^2-dG adducts in the 5′-TGC-3′ sequence paired with dC. The ^{32}P-labeled 24-mer primers positioning dC across from the adduct were annealed to 28-mer templates and incubated with KF in the presence of the next correct nucleotide (dATP), an incorrect dNTP (dTTP or dGTP), or all four dNTPs (as indicated) under conditions described under Materials and Methods. Aliquots were taken from the reaction mixture at the indicated time points, heated in the presence of formamide, and analyzed by denaturing PAGE (15%). The products were assigned in accordance with migration of standard oligonucleotides of identical sequences (not shown). Shown below, both the correct and misaligned primer-templates are predicted from the gel analysis.

primer extension reaction with all four dNTPs for 24 h. Presumably the misaligned structure in this case is more stable because two terminal bases of the primer 5′-TG-3′ can pair with downstream 5′-CA-3′ on the template (Figure 4C). This could result in some decrease of the extension efficiency observed in Figure 3A for the (+)-trans adduct paired with dT. When dG was positioned across from either the cis or the trans adduct (Figure 3A and Table 1), very low levels of extension in the presence of the next correct dNTP were observed (less than 8% after 1 h), suggesting that this mismatch provides significant inhibition of downstream replication, although the formation of a misaligned blunt-ended structure (Figure 4D) cannot be ruled out.

Analysis of Primer-Template Misalignments in the 5′-TGC-3′ Sequence. A similar set of experiments carried out with the 5′-TGC-3′ sequence indicated that misaligned structures may occur in this case. With the cis isomer paired with dC (Figure 7, top gel, and Table 4), incorporation of dAMP predominates (88% yield after 24 h), but significant levels (63% after 24 h) of dTMP (but not dGMP) are also incorporated, suggesting that a misalignment of the primer-template is possible. This misalignment is likely to be a minor component of the bypass process because in the presence of all four dNTPs only 4% of the total DNA in the reaction mixture after 24 h is a 27-mer, which would be the result of primer extension of this misaligned structure, whereas approximately 10% of the total DNA is the fully extended 28-mer. Interestingly, the fraction of misaligned primer-template in the case of the trans isomer appears to be greater than for the cis isomer (Figure 7, lower gel) since primer extension in the presence of dTMP, the next correct nucleotide for the misaligned primer-template, gives rise to an 11% yield of the 25-mer product after 24 h, which is comparable to the incorporation of dAMP, the next correct nucleotide for the correctly paired primer-template (8% yield after 24 h). However, the contribution of this structure on bypass cannot be evaluated fully because the level of full-length extension was negligible in this sequence. It is important to note that this potential misalignment structure did not result in increased levels of primer extension since the rate of replication in the presence of all four dNTPs was not faster in this sequence context than for the 5′-CGT-3′ sequence context where misalignment does not occur.

Analysis of the full-length extension reactions when a mismatched nucleotide is positioned across from the adduct (Figure 8) provides further evidence that this sequence is more prone to misalignments than the 5′-CGT-3′ sequence since in this case the 27-mer product of primer extension was detected. Interestingly, the extension in the presence of all four dNTPs when dA was positioned across from the (+)-trans adduct in this sequence was significantly more efficient than in any other case for either sequence context (Figure 8A and Table 4), such that the primer was almost completely extended after 24 h, giving rise mostly to the 27-mer product (85% of the total DNA in the reaction mixture) and only 9% of the 28-mer product. In the case of the cis adduct,

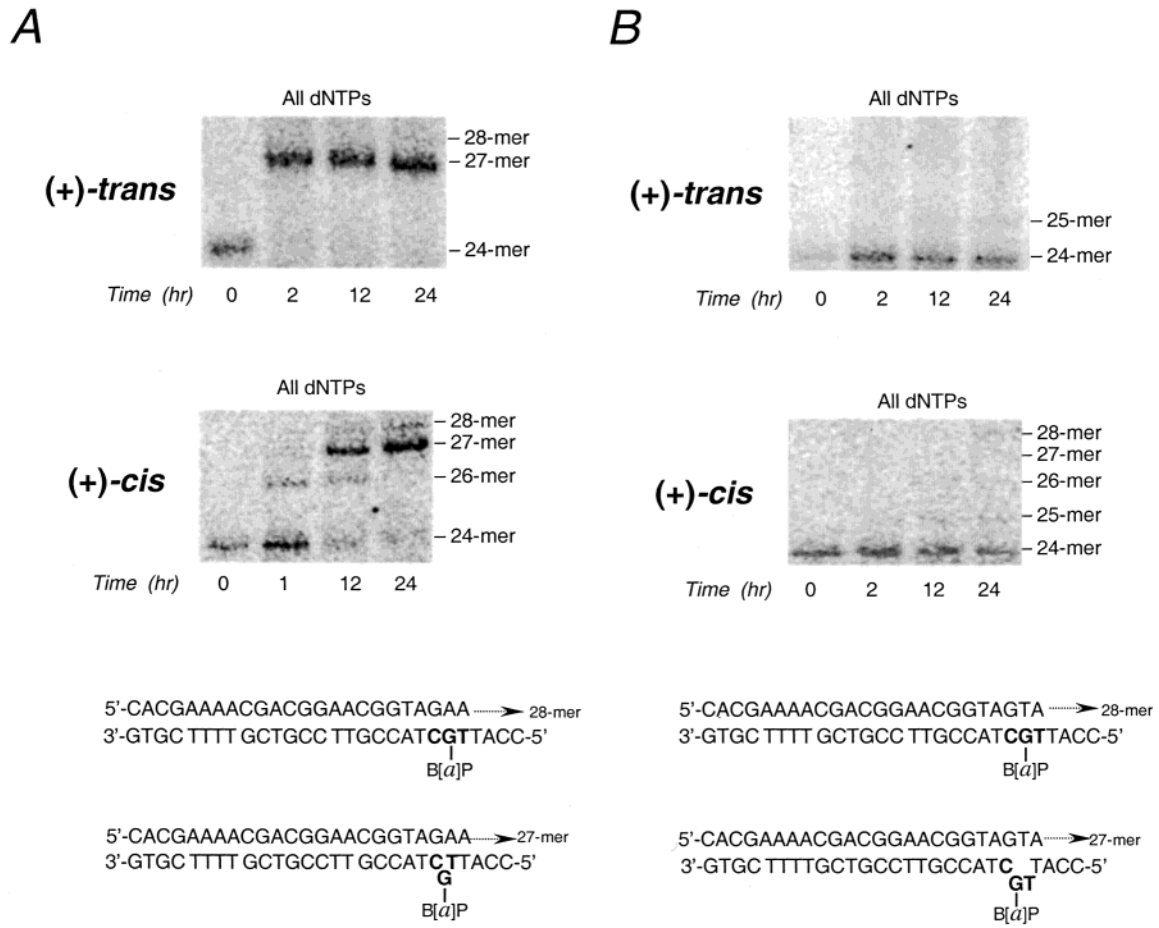

FIGURE 8: Full-length extension analysis of primer-templates containing the (+)-*cis*- or (+)-*trans*-B[*a*]P-N^2-dG adducts in the 5′-TGC-3′ sequence context. The ^{32}P-labeled 24-mer primers positioning dA (A) or dT (B) across from the adduct were annealed to 28-mer templates and incubated with KF in the presence of all four dNTPs under conditions described under Materials and Methods. Aliquots were taken from the reaction mixture at the indicated time points, heated in the presence of formamide, and analyzed by denaturing PAGE (15%). The products were assigned in accordance to migration of standard oligonucleotides of identical sequences (not shown). Appearance of the 27-mer product in accordance with the primer-template misalignment (as shown below) was observed when dA was positioned across from either adduct (A). No full-length extension was observed under the same reaction conditions when dT was positioned across from either adduct (B).

Table 4: Analysis of the Primer-Template Misalignment in the 5′-TGC-3′ Sequence

base across from adduct	adduct	incorporation of dAMP, %[a]	incorporation of dTMP, %[a]	fully extended product (28mer), %[b]	misalignment product (27mer), %[b]	alignment
C	(+)-cis	88	63	10	4	correct/incorrect
	(+)-trans	8	11	2	2	correct/incorrect
A	(+)-cis	nd[c]	nd	15	59	mostly incorrect
	(+)-trans	nd	nd	9	85	mostly incorrect
T	(+)-cis	nd	nd	6	5	correct/incorrect
	(+)-trans	nd	nd	not detected	not detected	nd

[a] Primer extension yields (%) in the presence of the next correct dNTP according to correct or incorrect alignment of the primer-template (dATP or dTTP, respectively, as shown in Figure 7, bottom) after 24 h of incubation. Primer extension yield (%) was calculated as the ratio of band intensity of the extension product to that of the total DNA (average of three independent experiments). The standard deviation in all cases did not exceed 15% and is omitted for clarity. Representative gels are shown in Figure 7. [b] Full-length primer extension yields (%) in the presence of all four dNTPs after 24 h of incubation were calculated as the ratio of band intensity of the full-length extension product (28-mer) or the product of full-length extension of the misaligned primer-template (27-mer, as shown in Figure 8, bottom) to that of the total DNA (average of three independent experiments). The standard deviation in all cases did not exceed 20% and is omitted for clarity. Representative gels are shown in Figures 7 and 8. [c] Not determined.

extension past the adduct occurred to a lesser extent than with the trans adduct (20% of the primer remained unextended after 24 h) and resulted in the production of both a 27-mer and a 28-mer (59% and 15% of the total DNA after 24 h, respectively). This suggests that the base-pairing of two consecutive A:T's resulted in a misaligned structure that was easily bypassed, especially in the case of trans adduct. Finally, consistent with the inefficient one-nucleotide extension with a dT positioned across from either adduct (Figure 3B), no full-length extension product was detected after 24 h incubation in the case of the (+)-trans adduct, and only 6% and 5% yields of the 28-mer and 27-mer, respectively (Figure 8B and Table 4), were observed for the (+)-cis adduct.

DISCUSSION

Effect of Adduct Stereochemistry on in Vitro Replication Bypass. The configuration of the bond between the B[*a*]P adduct and the guanine, rather than the stereochemistry of the hydroxyl groups on the aromatic ring, has been shown to influence in vivo DNA replication on templates containing these adducts (*11, 30*). This fact was one reason the (+)-trans and the (+)-cis adducts were chosen for the current and prior studies (*5, 21*), since these structures have an opposite configuration (10*S* and 10*R*, respectively) at this bond (Figure 1). However, previous in vitro studies, even though revealing significant quantitative differences in kinetic parameters of dNTP incorporation, showed that the overall trends were the same for each stereoisomer (*1, 5, 31*). For example, the insertion frequencies of nucleotide incorporation across from the adduct in 5′-CGC-3′, 5′-TGC-3′, and 5′-CGT-3′ sequence contexts followed the order: dA > dG > dT > dC, independent of adduct stereochemistry (*1, 5, 31*). A possible explanation for these results, based on the NMR structure of the (+)-trans adduct at a primer-template junction (*15*) and the computed structure of polymerase β bound to a (+)-*trans*-B[*a*]P-modified primer-template (*17*), is that the pyrenyl ring stacks with the adjacent base pair in the DNA duplex within the polymerase active site irrespective of the adduct stereochemistry, leading to a similar result when nucleotide incorporation occurs. In addition, we previously found that binding of KF to primer-templates containing a (+)-cis or (+)-trans adduct is similar when the primer terminated before the adduct position and that the presence of each of the dNTPs had comparable effects on this complex irrespective of adduct stereochemistry (*21*).

Although the inference from these results is that the polymerase interprets these different adduct structures similarly during the nucleotide incorporation step, which leads to similar nucleotide selectivity, there are clear differences that can be measured in the rates of extension by the polymerase from primer-templates containing these structures. Thus, we and others have found that the (+)-cis adduct is a much stronger block than the (+)-trans adduct both at the nucleotide insertion step (*1, 5, 31*) and for the addition of the next nucleotide past the adduct (*5*). The incorporation of this next nucleotide is apparently more difficult than the incorporation of the nucleotide across from the lesion (*1, 2, 5, 6, 29, 32*). The overall ability of the polymerase to extend the primer past the lesion, however, seems to depend on the sequence context and the identity of a nucleotide across from the adduct rather than on the stereochemistry of the adduct (*1, 5*).

An example where the stereochemistry of the adduct was shown to have qualitatively different effects is in the binding of the polymerase to primer-templates in which the primer extends up to the adduct position (*21*). The binding affinities varied significantly (up to the 6-fold difference) depending on the adduct stereochemistry and the identity of a nucleotide across from the adduct, providing the first evidence that the structures of these adducts within the active site of KF may be significantly different, even though the above-mentioned replication trends in the same primer-templates were the same (*5*).

These prior studies prompted us to carry out experiments using primer-template complexes in which the primer extended past the adduct position. Further rationale for this work is provided by recent structural studies with KF which have shown that there are important minor groove hydrogen-bonding interactions that take place between amino acids R668 and Q849 and the second base of the duplex region of the primer-template (*33*), the base that is modified in our experimental system (Figure 2, top). Both of these interactions have been proposed to be important for catalysis and fidelity (*33*). Similarly, a crystal structure of the large fragment of *B. stearothermophilus* DNA polymerase, which shares a large degree of homology with KF, indicates that there are extensive minor groove interactions with at least the first four base pairs of the duplex region (*34*). Thus, it seemed likely that positioning a bulky adduct of either stereochemistry in this region would substantially alter these interactions and that, because the adducts were located in a fully duplex region of the template, the adduct stereochemistry might effect these interactions, leading to measurable differences in the rates of DNA synthesis or polymerase binding.

The results obtained in the present studies indicated that the stereochemistry of the adduct does have a very strong effect on the incorporation of nucleotides at the +2 position (relative to the location of the adduct). It was found that although both adducts inhibited incorporation at this position, the (+)-trans adduct inhibited the downstream synthesis much more strongly than the (+)-cis isomer (Figures 2 and 3 and Table 1). These differences in the rates of extension are especially large when the Watson−Crick dC base is positioned across from the adduct in the 5′-CGT-3′ sequence: replication is essentially completely blocked in the case of (+)-trans adduct, whereas the primer is completely extended within 30 min in the case of the (+)-cis adduct (Figure 2A). This contrasts with what is found using the same templates for incorporation across from the adduct and extension directly from this position where the (+)-cis isomer has been found to be a stronger block (*5*).

The dramatic differences observed for the rates of primer extension at the +2 position suggest that the (+)-cis and (+)-trans adducts have very different structures once they are positioned within the duplex region of the DNA in the polymerase active site. The available structural information for these adducts in duplex DNA, at a primer-template junction, and within DNA polymerase active sites can be used to formulate a hypothesis that may explain these differences. In the case of the (+)-trans adduct, it has been shown that the pyrenyl ring lies in the minor groove directed in the 5′ direction both in duplex DNA and at a primer-template junction in which dC has been positioned opposite the modified guanine (*16, 35*). The modified base in both of these structures has been shown to retain the anti glycosidic torsion angle and has Watson−Crick hydrogen-bonded alignment with the complementary dC. Extending the primer by one nucleotide, as is the case for the primers used in the present study (Figure 2, top), would position the adduct deeper in the duplex region and thus should stabilize this structure. Moreover, because this structure is formed during the primer-template annealing, prior to interaction with KF, it might be retained upon the polymerase binding. If this were true, then it is likely that this structure would interfere with the above-mentioned important minor groove interac-

tions between the DNA and the polymerase that have been shown to be necessary for DNA synthesis (*34*).

In the case of the (+)-cis adduct, there are no structural data available that indicate where it is positioned at a primer-template junction. However, in a DNA duplex, the major conformer of this adduct has been shown to be intercalated between adjacent base pairs, causing the modified guanine to be displaced toward the minor groove and the partner cytosine toward the major groove (*36*). This structure is apparently stabilized by stacking interactions between the pyrenyl moiety and the adjacent base pairs. Even though the helix is distorted in the vicinity of the damage and guanine is displaced into the minor groove, it is possible that, were this conformation to be maintained within the polymerase active site in our experimental system, it would have a smaller effect on the overall geometry of the minor groove than in the case when the larger and more hydrophobic pyrenyl ring of the (+)-trans adduct is positioned in the minor groove (see Figures 11 and 12 in ref *14* for visual comparison). This potential structure might be expected to allow a higher rate of DNA synthesis downstream from the lesion. Other reasons, such as the probable greater conformational flexibility of the cis adducts (*14*), might also contribute to the observed differences, even though this would not explain why the (+)-cis adducts are stronger blocks of the replication across from and immediately past the lesion.

Effect of Sequence Context and Identity of the Nucleotide Incorporated Across from the Adduct on Replication Bypass. Previous studies involving the extension of the modified primer-templates in which the primer was terminated across from the adduct showed that the efficiency of extension past the lesion depends on the identity of the nucleotide positioned across from the adduct. It has been shown that in 5′-CGC-3′ (*1*), 5′-CGG-3′ (*2*), and 5′-TGC-3′ (*5*) sequences extension takes place only if dA is positioned across from the adduct, whereas in the 5′-CGT-3′ (*5*) sequence the extension past both the (+)-cis and (+)-trans adducts takes place mostly if not only when the primer terminates with dT across from the lesion. Results obtained by Zhuang and co-workers (*6*), however, were different and suggested that when the (+)-trans adduct was positioned within four different sequence contexts, including the previously studied 5′-CGC-3′ (*1*) and 5′-TGC-3′ (*5*), the best extension past the adduct was observed when dT was positioned across from the adduct in all cases. In both these sequences, Zhuang and co-workers found that when the primer was terminated by dT across from the adduct on the template, abnormally high insertion frequencies were observed for the incorporation of the next correct dNMP, with the rates comparable with those obtained using unmodified primer-templates. The authors (*6*) suggested that the observed efficient extension when the adduct is paired with dT for these two sequences is due to a misalignment mechanism. Conversely, we observed very efficient primer extension of 24-mer (Figure 8 and Table 4) and 23-mer primers (Figure S2, Supporting Information) in the presence of all four dNTPs when the adduct positioned within the 5′-TGC-3′ sequence is paired with dA and no bypass when the adduct is paired with dT. Formation of a 27-mer (−1 deletion) product in the case of dA suggests that the misaligned structures shown in Figures 8A (bottom) and S2A (bottom) are formed, which may facilitate the efficient bypass in this case. In general, the fact that bypass of the same lesion can occur producing such different results emphasizes the importance of the overall sequence context as opposed to the bases flanking the adduct.

As for the 5′-CGT-3′ sequence context, our results (*5*) and those of Zhuang and co-workers (*6*) are the same. In both studies, the extension was best when the adduct was paired with dT. We found that the extension frequencies determined for the (+)-trans and (+)-cis adducts (*5*) were very low [8.4×10^{-7} and 2.1×10^{-8}, respectively, not "very high" as stated in the discussion by Zhuang and co-workers (*6*)] whereas in the cases of other nucleotides positioned across from the adduct the extension was essentially not detectable in both studies. A detailed analysis suggests that in the case of the trans adduct paired with dT (see Figure S3, Supporting Information) the primer-template in our experiment might be indeed partially misaligned as proposed by Zhuang and co-workers (*6*). However, this analysis clearly shows that in the case of the cis adduct it is aligned correctly (see Figure S3, Supporting Information). Moreover, the partial misalignment observed in this sequence for the trans isomer did not cause an increase in the efficiency of replication bypass (Table 3 and Figures 6B and S3, Supporting Information), whereas misalignment observed in the 5′-TGC-3′ sequence when the adduct is paired with dA leads to relatively high rates of DNA synthesis (Table 4 and Figures 8A and S2A, Supporting Information).

Having mismatches at the modification sites also differently affects the primer extension downstream from the (+)-cis vs the (+)-trans adducts (Table 1 and Figure 3). At present, NMR data on how a mismatch would affect the conformation of the adduct are unavailable. Induced circular dichroism studies (*37*) suggest that the replacement of the hydrogen-bonding cytosine with a non-Watson−Crick dC base leads to formation of intercalative conformations in the case of the (+)-trans adduct. In accordance with the model proposed above, this might explain the observed trend that the primer extension downstream from the lesion was faster when the adduct was paired with a mismatched base rather than with Watson−Crick dC (Table 1 and Figure 3). Alternatively, in the case of the (+)-cis adduct, where the conformation of the adduct is expected to be intercalative, the displacement of the more bulky purine into the major or minor groove might result in greater hindrance during replication than would be found with a displaced pyrimidine, thus decreasing the replication rates as observed (Table 1 and Figure 3A) for the 5-CGT-3′ sequence, which is less affected by primer-template misalignment.

The identities of the nucleotide across from the adduct that were optimal for the replication downstream from the lesion were different for the (+)-cis and (+)-trans adducts (Figure 3 and Table 1), which might differentially contribute to the mutagenic bypass of these lesions. This is the first indication from in vitro studies that the adduct stereochemistry may favor different base substitution mutations. All prior studies, which measured the rates of incorporation across from the adduct or extension one nucleotide past the adduct, gave comparable results for both adduct stereochemistries (*1, 5*). It is interesting to note that the (+)-cis adduct has shown higher levels of mutagenicity in *E. coli* than the (+)-trans adduct (*12*). It is possible that this effect may be partially attributed to the fact that the cis adduct inhibits

downstream replication less than the trans adduct, which would compensate for the stronger inhibition observed for incorporation of a dNTP at or immediately past the adduct site. A detailed explanation of the observed trends awaits three-dimensional structural studies of the adduct conformations in different sequences with or without possible mismatches and possibly within the active site of a polymerase.

Consistent with what was found for the primers one nucleotide shorter [(*5*) and Figure S2, Supporting Information], having a dT across from the adduct is more favorable in the case of the 5′-CGT-3′ sequence (Tables 1 and 3, Figure 3A, and cf. Figure 6A,B), whereas in the 5′-TGC-3′ sequence extension past the adduct paired with dT is poor in the case of both stereoisomers (Tables 1 and 4, Figure 3B, and cf. Figure 8A,B). In general, the downstream primer extension by one nucleotide was more efficient in the 5′-CGT-3′ sequence than in the 5′-TGC-3′ sequence (Table 1, Figures 2 and 3). The observed differences in efficiencies of the primer extension reactions may be at least partially related to the fact that in the 5′-CGT-3′ sequence the G:C base pair positioned on the border of the double-stranded/single-stranded regions in the primer-templates stabilizes the overall structure better than does the A:T base pair in the 5′-TGC-3′ sequence, which may result in an increase in the adduct conformational freedom and lead to formation of a misaligned primer-templates in the latter case. Based on the modeling studies, it has been proposed that different conformations of the adduct are favored in different sequence contexts including the ones studied here (*8*, *19*), which may also account for the differences observed in the present study.

Effects of the Sequence Context and Stereochemistry of the Adduct on Primer-Template Misalignment. Analysis of primer-templates in two sequence contexts with all four possible nucleotides across from the adduct suggests that reasonably stable primer-template misalignments can be formed if at least two terminal bases of the primer can base-pair with two consecutive bases on the template downstream of the lesion. The data from Zhuang and co-workers (*6*) suggest that looping of a rather long portion of the template containing the (+)-*trans*-*anti*-B[*a*]P-N^2-dG adduct can occur within the polymerase active site. Not surprisingly, we found that the 5′-CGT-3′ sequence, having a more stable G:C base pair on the terminus of the double-stranded portion of the primer-template, was aligned correctly in most cases, although some levels of misalignment were detected in the case of the (+)-trans adduct paired with dT. The 5′-TGC-3′ sequence, however, was shown to be more prone to misalignments, and, more importantly, the misalignment in the case when the adduct was paired with dA significantly affected the replication bypass of the lesion, leading to very efficient formation of a product with −1 deletion. This result was consistent with a previous in vitro study of Shibutani (*1*), where a 9-fold increase of the replication products containing a −1 deletion was detected in this sequence compared with the 5′-CGC-3′ sequence, and the study by Bernelot-Moens (*38*) in which formation of −1 deletions was detected in vivo in the 5′-TG-3′ sequence.

Interestingly, in each case studied, the propensity for the cis adducts to promote the formation of the misaligned primer-templates was much lower than for the trans adducts (see Tables 3 and 4). This finding is rather surprising since it was predicted that the helix-distorting cis adducts should promote the misalignments more than extrahelical trans adducts (*1*). It is possible that the stacking of the pyrenyl ring with the adjacent base pairs compensates for the helix distortion and stabilizes the correctly aligned structures in the case of the cis adducts (*14*). In addition, the stability of the duplex DNA containing the cis adducts was found to be higher (which results in 4−5° C higher melting temperatures) than that containing the extrahelical trans adducts (*14*).

In summary, in the absence of sufficient structural or computational data on the conformations of the bulky adducts within the active site of polymerase, this study provides strong direct evidence that the structures of the (+)-cis and (+)-trans adducts are significantly different after the modified primer-template is bound by KF. Presumably, the presence of these different structures leads to very different primer extension efficiencies. We predict that the structure of the (+)-trans adduct when positioned in the double-stranded part of the primer-template junction resembles that found in the full duplex, where the pyrenyl ring is situated in the minor groove. In this conformation, it would likely cause significant steric hindrance and disrupt important minor groove interactions within the polymerase active site. Alternatively, we propose that the (+)-cis adduct retains the intercalated structure within the active site and that this structure, even though being a stronger block at the site of the lesion, is more suitable for downstream extension. Finally, we found that the trans adducts are more able to promote formation of primer-template misalignment compared with the cis adduct in identical sequence contexts. Thus, even though the (+)-cis adduct is a stronger block of the nucleotide incorporation across from and just past the lesion, its effect on downstream replication is significantly less compared with the (+)-trans adduct, factors that may contribute to the relative mutagenicity of each species.

ACKNOWLEDGMENT

We thank Dr. Mohsen B. Arghavani for synthesizing the (±)-*anti*-B[*a*]PDE-modified 11-mer oligonucleotides.

SUPPORTING INFORMATION AVAILABLE

Three additional figures are included. This material is available free of charge via the Internet at http://pubs.acs.org.

REFERENCES

1. Shibutani, S., Margulis, L. A., Geacintov, N. E., and Grollman, A. P. (1993) *Biochemistry 32*, 7531−7541.
2. Hanrahan, C. J., Bacolod, M. D., Vyas, R. R., Liu, T., Geacintov, N. E., Loechler, E. L., and Basu, A. K. (1997) *Chem. Res. Toxicol. 10*, 369−377.
3. Keohavong, P., Shukla, R., Melacrinos, A., Day, B. W., and Reha-Krantz, L. (1998) *DNA Cell Biol. 17*, 541−549.
4. Lipinski, L. J., Ross, H. L., Zajc, B., Sayer, J. M., Jerina, D. M., and Dipple, A. (1998) *Int. J. Oncol. 13*, 269−273.
5. Alekseyev, Y. O., and Romano, L. J. (2000) *Biochemistry 39*, 10431−10438.
6. Zhuang, P., Kolbanovskiy, A., Amin, S., and Geacintov, N. E. (2001) *Biochemistry 40*, 6660−6669.
7. Seo, K. Y., Jelinsky, S. A., and Loechler, E. L. (2000) *Mutat. Res. 463*, 215−246.
8. Kozack, R., Seo, K. Y., Jelinsky, S. A., and Loechler, E. L. (2000) *Mutat. Res. 450*, 41−59.
9. Harvey, R. G. (1991) *Polycyclic Aromatic Hydrocarbons: Chemistry and Carcinogenicity*, Cambridge University Press, Cambridge, U.K.

10. Denissenko, M. F., Pao, A., Tang, M., and Pfeifer, G. P. (1996) *Science 274*, 430−432.
11. Moriya, M., Spiegel, S., Fernandes, A., Amin, S., Liu, T., Geacintov, N., and Grollman, A. P. (1996) *Biochemistry 35*, 16646−16651.
12. Fernandes, A., Liu, T., Amin, S., Geacintov, N. E., Grollman, A. P., and Moriya, M. (1998) *Biochemistry 37*, 10164−10172.
13. Newbold, R. F., and Brookes, P. (1976) *Nature 261*, 52−54.
14. Geacintov, N. E., Cosman, M., Hingerty, B. E., Amin, S., Broyde, S., and Patel, D. J. (1997) *Chem. Res. Toxicol. 10*, 111−146.
15. Cosman, M., Hingerty, B. E., Geacintov, N. E., Broyde, S., and Patel, D. J. (1995) *Biochemistry 34*, 15334−15350.
16. Feng, B., Gorin, A., Hingerty, B. E., Geacintov, N. E., Broyde, S., and Patel, D. J. (1997) *Biochemistry 36*, 13769−13779.
17. Singh, S. B., Beard, W. A., Hingerty, B. E., Wilson, S. H., and Broyde, S. (1998) *Biochemistry 37*, 878−884.
18. Perlow, R. A., and Broyde, S. (2001) *J. Mol. Biol. 309*, 519−536.
19. Kozack, R. E., Shukla, R., and Loechler, E. L. (1999) *Carcinogenesis 20*, 95−102.
20. Dzantiev, L., and Romano, L. J. (1999) *J. Biol. Chem. 274*, 3279−3284.
21. Alekseyev, Y. O., Dzantiev, L., and Romano, L. J. (2001) *Biochemistry 40*, 2282−2290.
22. Dzantiev, L., and Romano, L. J. (2000) *Biochemistry 39*, 5139−5145.
23. Kunkel, T. A., and Bebenek, K. (2000) *Annu. Rev. Biochem. 69*, 497−529.
24. Derbyshire, V., Freemont, P. S., Sanderson, M. R., Beese, L., Friedman, J. M., Joyce, C. M., and Steitz, T. A. (1988) *Science 240*, 199−201.
25. Maniatis, T., Fritsch, E. F., and Sambrook, J. (1982) *Molecular Cloning. (A Laboratory Manual)*, Cold Spring Harbor Laboratory Press, Cold Spring Harbor, NY.
26. Arghavani, M. B., SantaLucia, J., Jr., and Romano, L. J. (1998) *Biochemistry 37*, 8575−8583.
27. Shibutani, S., Takeshita, M., and Grollman, A. P. (1991) *Nature 349*, 431−434.
28. Shibutani, S., and Grollman, A. P. (1993) *Chem. Res. Toxicol. 6*, 819−824.
29. Miller, H., and Grollman, A. P. (1997) *Biochemistry 36*, 15336−15342.
30. Shukla, R., Jelinsky, S., Liu, T., Geacintov, N. E., and Loechler, E. L. (1997) *Biochemistry 36*, 13263−13269.
31. Mekhovich, O. (1997) in Ph.D. Dissertation, Wayne State University, Detroit, MI.
32. Shibutani, S., and Grollman, A. P. (1993) *J. Biol. Chem. 268*, 11703−11710.
33. Spratt, T. E. (2001) *Biochemistry 40*, 2647−2652.
34. Kiefer, J. R., Mao, C., Braman, J. C., and Beese, L. S. (1998) *Nature 391*, 304−307.
35. Cosman, M., de los Santos, C., Fiala, R., Hingerty, B. E., Singh, S. B., Ibanez, V., Margulis, L. A., Live, D., Geacintov, N. E., Broyde, S., and Patel, D. J. (1992) *Proc. Natl. Acad. Sci. U.S.A. 89*, 1914−1918.
36. Cosman, M., de los Santos, C., Fiala, R., Hingerty, B. E., Ibanez, V., Luna, E., Harvey, R., Geacintov, N. E., Broyde, S., and Patel, D. J. (1993) *Biochemistry 32*, 4145−4155.
37. Pradhan, P., Jernstrom, B., Seidel, A., Norden, B., and Graslund, A. (1998) *Biochemistry 37*, 4664−4673.
38. Bernelot-Moens, C., Glickman, B. W., and Gordon, A. J. (1990) *Carcinogenesis 11*, 781−785.

BI015850L